

Soft Matter

Accepted Manuscript



This is an *Accepted Manuscript*, which has been through the Royal Society of Chemistry peer review process and has been accepted for publication.

Accepted Manuscripts are published online shortly after acceptance, before technical editing, formatting and proof reading. Using this free service, authors can make their results available to the community, in citable form, before we publish the edited article. We will replace this *Accepted Manuscript* with the edited and formatted *Advance Article* as soon as it is available.

You can find more information about *Accepted Manuscripts* in the [Information for Authors](#).

Please note that technical editing may introduce minor changes to the text and/or graphics, which may alter content. The journal's standard [Terms & Conditions](#) and the [Ethical guidelines](#) still apply. In no event shall the Royal Society of Chemistry be held responsible for any errors or omissions in this *Accepted Manuscript* or any consequences arising from the use of any information it contains.

Cite this: DOI: 10.1039/c0xx00000x

www.rsc.org/xxxxxx

ARTICLE TYPE

The position of hydrophobic residues tunes peptide self-assembly

Christian Bortolini,^{a,b} Lei Liu,^{a,c} Thomas M. A. Gronewold,^d Chen Wang,^b Flemming Besenbacher^a and Mingdong Dong^{*a}

Received (in XXX, XXX) Xth XXXXXXXXX 20XX, Accepted Xth XXXXXXXXX 20XX

DOI: 10.1039/b000000x

The final structure and properties of synthetic peptides mainly depend on their sequence composition and experimental conditions. This work demonstrates that a variation in the positions of hydrophobic residues within a peptide sequence can tune the self-assembly. Techniques employed are atomic force microscopy, transmission electron microscopy and an innovative method based on surface acoustic waves. In addition, a systematic investigation on pH dependence was carried out by utilizing constant experimental parameters.

Synthetic amphiphilic peptide self-assembly^{1, 2} is a hot topic in nanoscience. The outstanding ability of these peptides to arrange into well-organized nanostructures^{3, 4} has allowed a deep understanding of the natural peptide assembly (e.g. amyloid fibrils).⁵⁻⁷ By mimicking natural sequences and by trying to replicate the *in vivo* environment, it is possible to obtain information concerning the dynamics of their self-assembly (e.g. fibrillation process⁸⁻¹⁰, cytotoxicity studies¹¹⁻¹³, and other disease related kinetics). This research opens up a broad variety of intriguing potential applications, e.g. nanomaterials, sensing devices¹⁴. The specific sequence and the particular amino acids chosen for the peptide composition determine the final structures and, thus, the properties of the peptides^{15, 16}. Furthermore, it is known that by changing pH,¹⁷ incubation shaking speed¹⁸ or other experimental and environmental conditions, the peptides fold into different secondary and tertiary structures. The pH changes will lead to the change of assembly due to tuning the peptide charge. However, for peptides with the same amino acid sequence is that the order of amino acids does not change the charge. This work shows that even when the residues are maintained and at constant experimental parameters, it is possible to turn the assembled structures by changing the positions of the hydrophobic residues within the sequence.

Three short sequences with nine amino acids were designed, which consist of a hydrophobic part of two phenylalanine-alanine repeats (inspired by the β -amyloid(1-40) sequence¹⁹), and a hydrophilic part with in total four serines and one cysteine. Figure 1 presents the three molecular models (called **P1**, **P2** and **P3** respectively) and the peptide charge chart, which is the same for all peptides since the amino-acids involved are the same. The polar region is highlighted since it is directing²⁰ the self-assembly toward specific secondary structures and specific structure formation. It is worth to notice that the C-termini of all the three

sequences are amidated. In such a way no C-terminus is involved in the self-assembly process.

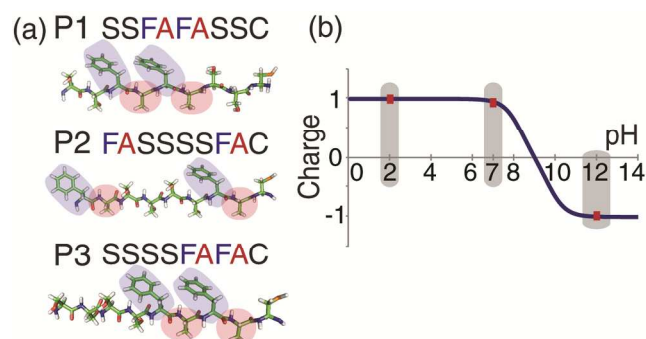


Fig. 1 Molecular models of the designed three peptides (a) with the same charge chart (b). The three pH values (2, 7, 12) at which measurements have been performed are highlighted.

Hydrophobic residues of **P1** (FAFA) are located in the center, separated from the termini by at least two polar amino acids (see Fig. 1a). In **P2**, two FA pairs surround a hydrophilic core of four serines SSSS. **P3** possesses on the one side an N-terminal polar region and on the other side a non-polar region. This makes the monomer perfectly amphiphilic (i.e. the charge is completely separated and thereby maximal effective).

Figure 1b presents a peptide charge chart. Above pH 7 the charge drops to negative values, while below pH 7 the charge is positive. Thus, we expect that a neutral and a low pH promotes the self-assembly of monomers into well-organized nanostructures. Three pH values have been chosen for the analysis: pH 2, pH 7 and pH 12 (highlighted in grey in Fig. 1b). It is known that a low pH provides the best conditions for the self-assembly of amyloids first into proto-filaments and finally can form fibrils.^{17, 21} Peptide sequences utilized in this work are designed to be amyloid-like thereby promoting such structures. On the other hand, the formation of well-ordered nanostructures is not promoted at high pH.

Figure 2 shows Atomic Force Microscopy (AFM) topographical images of **P1** at three pH values, height profiles referred to these images and an estimation of the coverage. At pH 2 (Fig. 2a) peptides arranged on the mica surface following hexagonal symmetry.²² Most likely, interactions between different units (pre-formed in solution) are weaker than the interaction within the hydrophilic mica surface which has a hexagonal pattern as it has been observed²³ previously. This provides information about

the equilibrium of the system and about the self-assembly driving forces. In particular, Van der Waals forces are established between the substrate and the phenyl rings of phenyl-alanines (2 per monomer) driving the sheet-like structures toward hexagonal symmetry arrangement rather than an arbitrary disposition²⁴ – see *Figures S4 and S5 in Supporting Information*. *Figure S4* shows AFM images exhibiting the hexagonal symmetry arrangement of sheet-like structures; *Figure S5* presents a comparison between the Fourier transform images of **P1** fibrils and sheet-like structures highlighting the hexagonal symmetry of the latter. In addition, to further support this hypothesis, i.e. sheet-like structures arrange once landed on the surface, it is expected that the coverage is dependent on the deposition time (since there is more time for sheet-like structures to arrange and to be attracted by the surface). *Figure S6* in Supporting Information shows that by varying the deposition time it is possible to tune the coverage by going from nearly 0.5 monolayers (ML) to a 0.9 ML film.

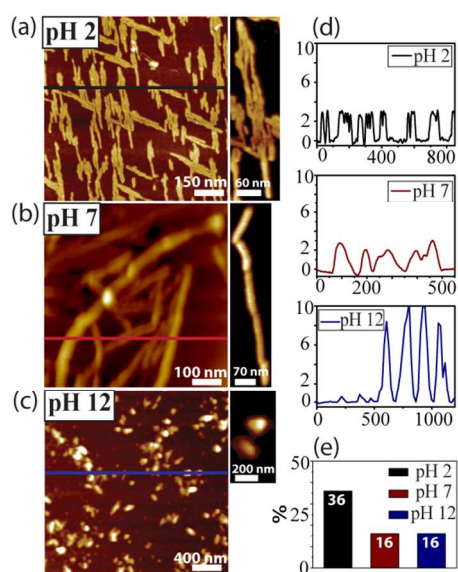


Fig. 2 AFM topography images of **P1** respectively at: pH 2 (a), pH 7 (b) and pH 12 (c); on the right-hand side is shown a representative sample for the structure. (d) Height profiles: black line and profile = pH 2, red = pH 7 and blue = pH 12. (e) Histograms showing the coverage percentage, according to the same color legend.

The height is around 3 nm in the range of elongated sheet-like structures²². The analysis at pH 7 reveals the formation of several amyloid-like fibrils²⁵ resulting in a distribution of sizes²⁶. *Fig. 2b* presents the dominant fibril structure that has been observed. The height is similar to the sheets (pH 2) but without any relation between the fiber disposition on the surface and the crystallographic properties of the mica substrate. The fibril polymorphism observed in amyloids was also present in our analysis,²⁶⁻²⁹ thus, it is important to define a dominant structure. At pH 12 only particles are revealed even by gentle heating of the peptide during incubation or by increasing the number of incubation days (*Fig. 2c*). The height of these particle structures was 8 nm up to 10 nm which is almost three times higher than the nanostructures formed at lower pH 2 and pH 7. Monomers prefer to randomly appose forming globular structures instead of self-assemble in an ordered and hierarchical manner. The coverage

computation (*Fig. 2d*) reveals that a higher amount of monomer participated in the self-assembly to sheets at pH 2 than the 16% at both pH 7 and pH 12. At pH 7, some monomers participate in the self-assembly but only formed tiny fibrils which were excluded from the calculation (however visible at TEM, as shown in *Figure S7a in Supporting Information*). Thus, the value at pH 7 is a little underestimated and it is expected to be approximately 5-10% higher.

The core hydrophobic FAVA group is the leading region of the peptide for the self-assembly^{30, 31}. We investigated its influence by making a sequence in which the FAVA group is split and separated (**P2** peptide) by a thick core of several hydrophilic, non-polar serines. **P2** possesses the sequence FASSSFAC. Phenyl-alanine (F) and cysteine (C) are both N-termini. *Figure 3* presents AFM topographical images of **P2**, height profiles referred to these images and an estimation of the coverage. Since the hydrophobic interactions are the driving force for the amphiphilic peptide self-assembly, it is expected that by changing the position of these residues, the arising structures differ. In fact, at pH 2 (*Fig. 3a*), fibrils were formed and not sheets. These fibrils are small (see also *Figure S1 in Supporting Information*) compared to the sheets formed by **P1** (pH 2) and this characteristic is reflected in the average height which is only about 1.8 ± 0.3 nm.

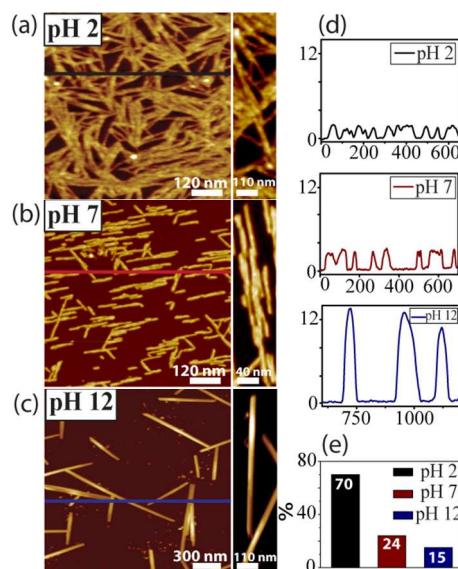


Fig. 3 AFM topography images of **P2** respectively at: pH 2 (a), pH 7 (b) and pH 12 (c); on the right-hand side is shown a representative sample for the structure. (d) Height profiles: black line and profile = pH 2, red = pH 7 and blue = pH 12. (e) Histograms showing the coverage percentage, according to the same color legend.

Surprisingly, at pH 7 (*Fig. 3b*) sheets were formed. Similar to the sheets formed by **P1** at pH 2 both their height and the effect of the surface are acting as hexagonal template at deposition. *Fig. 3c* (and *Figure S2 in Supporting Information*) shows that at pH 12 monomers self-assemble in rod-like aggregates 12 ± 2 nm tall. The rod width is highly similar for the individual units measured at 40 ± 2 nm, whereas the length ranges from 500 nm and 1 μ m. The coverage gradually decays from low pH to higher pH. The coverage follows a trend similar to the previous sequence (see *Fig. 2e*). Moreover, the mica surface can interfere with the

disposition of pre-formed structures (**P1**: sheets at pH 2; **P2**: sheets at pH 7 and rods at pH 12). This can be explained by lower interactions between individual units than the already relatively weak attraction force provided by the mica. In addition to the AFM investigation, a closer inspection by Transmission Electron Microscopy (TEM) offered a wider sample overview (see *Figures S1 and S2 in Supporting Information* for **P2** structures at pH 2 and pH 12). TEM images of different fibers obtained at pH 2 for **P2** and at pH 7 for **P1** are summarized in *Figures S7a and S7b in Supporting Information*. TEM analysis can provide detailed information that cannot be extracted using AFM, such as fiber's width. An estimation of this parameter is presented in *Table S1 in Supporting Information*. Sheet-like structure TEM image is shown in *Figure S8 in Supporting Information*.

In order to obtain the information on the secondary structure Synchrotron Radiation Circular Dichroism (SR-CD) spectra of **P2** structures formed at pH 2 (fibrils of *Fig. 3a*) and pH 7 (sheet-like structures *Fig. 3b*) are shown in *Figure S9 in Supporting Information*. Fibrils spectrum (black line in *Fig. S9*) exhibits three main peaks at 191 nm, 198 nm and 217 nm respectively. Sheet-like structures spectrum (red line in *Fig. S9*) presents similar peaks at 191 nm, 198 nm and 220 nm. Spectra suggest the predominance of random coil secondary structures both for pH 2 and pH 7 samples. However, by comparing these two spectra, it is observed that the third peak of pH 7 sheet-like structures at 220 nm is located at higher values respect to the fibrils one which was 217 nm, indicating that a change in secondary structure occurred at the high pH.

We investigated the case in which the hydrophobic residues (FAFA) are located in the center of the sequence, separated from the termini by at least two polar amino acids (**P1**), then we investigated the case in which the FAFA group is split and separated (**P2**) by four hydrophilic serines. Now, it may be interesting to consider the case in which the FAFA group stays together and it is just shifted to a different position from the original sequence **P1**. For this purpose we designed and investigated a new sequence, **P3** SSSSFAFAC. Serine (S) and cysteine (C) are both N-termini. The FAFA group is neither split nor embedded in non-polar residues, but surrounded by two well-defined regions with opposite polarity. *Figure 4* shows AFM topographical images of **P3**, height profiles referred to these images and an estimation of the coverage. A low pH promotes self-assembly into fibrils. *Fig. 4a* shows peptide fibers that are almost twice the sizes of **P1**'s fibrils and triple of the fibrils formed by **P2**.

At pH 7 fibrils are formed with a highly differing structure. The height is comparable with those formed by **P1** at same pH, but the shape is unique. *Fig. 4b* shows that these fibrils appear to be very flexible. They can even arrange in circles exhibiting a very short persistence length (i.e. the fibrils tendency to bend is very high). TEM images of **P3** fibers obtained at pH 2 and pH 7 are shown in *Figures S7c and S7d in Supporting Information*. At pH 12 bow-like sheets structures are formed (*Fig. 4c*). The height is 2.2 ± 2.0 nm, the length ranges from 500 nm to 900 nm, the width is 30 ± 10 nm at the thin part and 60 ± 10 nm at the thickest.

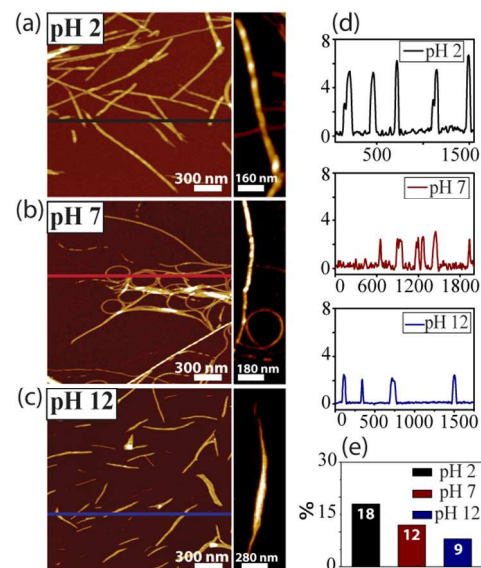


Fig. 4 AFM topography images of **P3** respectively at: pH 2 (a), pH 7 (b) and pH 12 (c); on the right-hand side is shown a representative sample for the structure. (d) Height profiles: black line and profile = pH 2, red = pH 7 and blue = pH 12. (e) Histograms showing the coverage percentage, according to the same color legend.

These structures appear after one week incubation time, while the previously presented structures were formed within two days of incubation. Structures of **P3** are significantly different from the other two sequences and the coverage is lower than the structures formed by **P1** and **P2**. When the results of three peptides are compared, we can conclude that the position of the hydrophobic residues plays a crucial role in directing the self-assembly toward specific pathways. In the cysteine-rich peptides considered in this work, the pH seems a sort of limiting factor. When the charge is negative the formation of fibrils and sheets is strongly disfavored. On the contrary, when the monomer charge is positive (see *Fig. 1b*) interactions among monomers are promoted leading to formation of sheets or fibrils.

Moreover, being our sequences cysteine-rich, disulfide bond formation is likely to occur and affect the peptide self-assembly. In particular, at pH 12, such a basic pH will probably lead to lantibiosation of the peptide.

Figure 5 summarizes the findings resulting from the AFM analysis by showing the coverage and the height values for each monomer at the three pH values used. In the height profiles (*Fig. 5a*), the height value is homogeneous at pH 7 and increases when pH 12 structures are formed. In the coverage profiles (*Fig. 5b*), the coverage decreases at increasing pH value, thus, they are inversely proportional. Structures arising at different pH values with different sequences are summarized in *Table 1*.

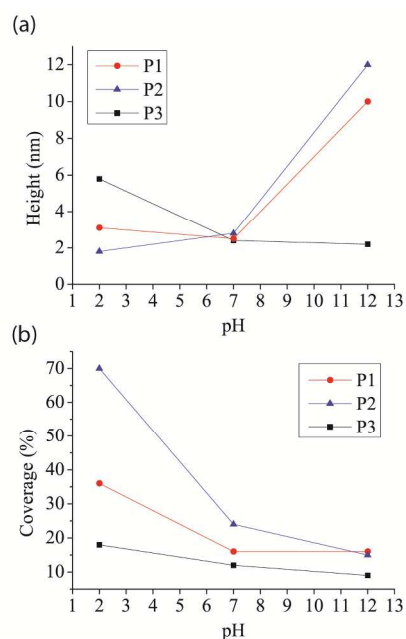


Fig. 5 Graphics summarizing the AFM analysis by correlating the three monomers dependence on the pH either versus the height (a) and the coverage (b), respectively.

	Sequence	pH 2	pH 7	pH 12
P1	SSFAFASSC	sheets	fibrils	particles
P2	FASSSFAC	fibrils	sheets	rods
P3	SSSFAC	fibrils	fibrils	sheets

Table 1 Summary of structures forming at different pH values for different peptides (P1, P2 and P3).

In order to obtain further insights into the dynamics of the self-assembly, a new technique has been exploited. Basically, peptide binding to the surface was analyzed with a samX surface acoustic wave (SAW) biosensor (SAW instruments, Bonn, Germany) (i.e. chip surface modifications), using the modulation of a surface confined acoustic wave. Phase and amplitude of the wave correspond to mass loading and viscoelastic properties on the surface, respectively.

The SAW technology is a valid alternative to Quartz Crystal Microbalance with Dissipation monitoring (QCM-D)^{32, 33}, since the SAW technology possesses a higher sensitivity and enables combination of multiple sensor elements on a single chip. In our experiment with P3, four channels on a chip with a gold surface have been used. The experiment consisted of incubating P3 in monomeric form and in pre-formed (but ultra-sonicated) fibrils in double-distilled water (ddH₂O) on a gold chip, at a flow rate of 12.5 μl/min and 0 μl/min. Aim was to follow the dynamics of fibrillation for approximately 2 days.

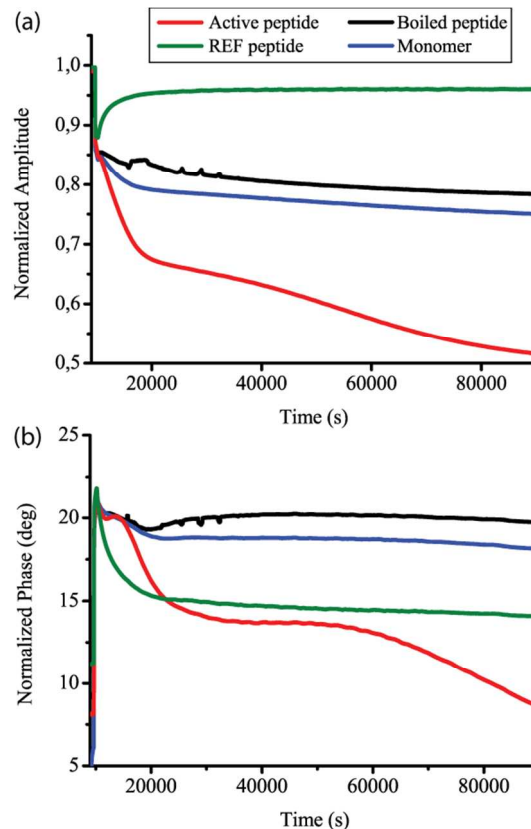


Fig. 6 Detail of a SAW measurement of P3. Time is in abscissa and the variation of the phase is in ordinate. Color coded lines show the phase variation for 4 different compounds. P3 was injected into running double-distilled water (ddH₂O) directly followed by a 24 hour incubation period at 0 flow with P3 solution until 90,000 s. Appreciable changes are visible only in the case of Active peptide (red line).

Figure 6 shows an exemplary SAW measurement on P3 fibrils reacting with different surfaces. The four elements on the SAW chip were modified with (i) P3 fibrils that have been ultra-sonicated and boiled (i.e. denatured) for 2 hours (channel 1, black line), (ii) P3 the unaltered monomer (channel 2, blue line), (iii) freshly ultra-sonicated P3 fibrils (channel 3, red line) and (iv) a reference peptide (REF peptide) employed to check the presence of artefacts, with the sequence TRQARRRRRWRER (channel 4, green line). Figure S3 in Supporting Information shows the complete measurement (both amplitude and phase signals) of the experiment. Basically, the injected P3 solution was incubated for 24 hours at 0 μl/min with the different surfaces on the chip without supply of fresh P3, followed by the progression at flow rate 12.5 μl/min for another 24 hours. The most interesting part is the incubation period between 15,000 s and 90,000 s. While the signals on the monomer, denatured peptide and reference surface are not changing and the mass-viscoelasticity relationship is linear, there is a clear decrease in the phase and damping of the amplitude signal (see Fig. 6b). We assume that this relationship between mass loss and increase in viscoelasticity is an indication of the ongoing fibrillation process provoked by the P3 fibril fragments. Interestingly, on the monomer surface no such significant modification in conformation and mass on the chip surface were detected compared to the sonicated fibrils (termed “active peptide”). This modification can be divided into 3 steps: (1) the signal is lowering very rapidly below 20,000 s; (2)

between 20,000 s and 60,000 s (nearly 12 hours) a plateau is reached and (3) above 60,000 s, in which the signal slowly decreases. An interpretation of such behaviors is that the freshly sonicated fibrils (active peptide) act as seeds that rapidly self-assemble by attaching to each other. Once no additional seeds are available, a lag phase is lasting for approximately 12 hours (plateau in the measurement, Fig. 6 red line). Then, the fibrils gradually continue to elongate, probably by using the monomers that remain free in solution and are still available, or rearrange as depicted in Fig. 4b. Such a behavior also is typical for amyloid fibrils³⁴, but these results provide new insights about timing of each specific dynamic process.

Conclusions

In this work we show that the hydrophobic residues can direct the peptide self-assembly toward the formation of different nanostructures. This discovery gives new interesting insights about the peptide self-assembly helping to solve open issues about the folding of medical (or device related) relevant peptides (e.g. amyloids). Moreover, by keeping constant all the experimental and environmental conditions and by varying just sequence or pH, the role of the pH in the self-assembly has been clarified. To elucidate the dynamics of the fibril self-assembly, the innovative SAW technique has been employed. The same approach can be applied to other peptides opening future perspectives for insights in peptide self-assembly regarding specific dynamics such as lag phase and seeding timing. For instance, cytotoxicity studies often relies on the choice of a specific sequence that scientist considered to be toxic or promoting the onset of a specific disease, regardless the particular position of the residues.

Acknowledgements

This work was supported by grants from the Danish National Research Foundation and the Danish Research Agency through support for the iNANO Center. M.D. acknowledges a STENO Grant for the Danish Research Council and the VKR Young Investigator Program in Denmark. C.B. acknowledges PhD Scholarship from Sino-Danish Center for Education and Research.

Notes and references

^a *Interdisciplinary Nanoscience Center (iNANO), Gustav Wieds 14, Building 1590, Aarhus C., Denmark. Fax: +45 8715 4041; Tel: +45 8715 0000; E-mail (MD): dong@inano.au.dk*

^b *National Center for Nanoscience and Technology (NCNST), No. 11, Beiyitiao Zhongguancun, Beijing, P. R. China. Fax: +86 10-62656765; Tel: +86 10-82545545.*

^c *Institute For Advanced Materials, JiangSu University, China*

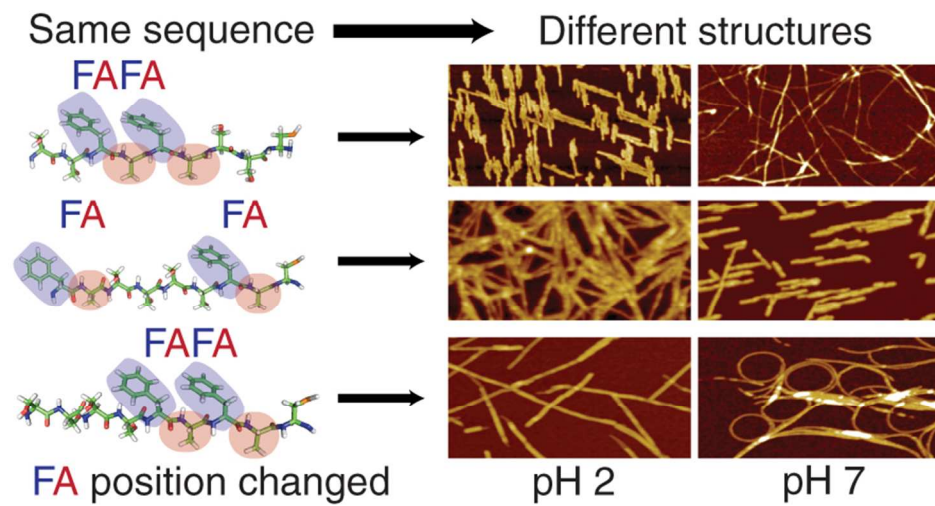
^d *SAW Instruments GmbH Schwertberger, Str. 16, 53177 Bonn, Germany: +49 (0) 228 / 812 876-20; Tel: +49 (0) 228 / 812 876-13.*

[†] Electronic Supplementary Information (ESI) available: [details of any supplementary information available should be included here]. See DOI: 10.1039/b000000x/

1. I. W. Hamley, *Soft Matter*, 2011, **7**, 4122-4138.

2. H. Cui, M. J. Webber and S. I. Stupp, *Peptide Science*, 2010, **94**, 1-18.
3. R. V. Ulijn and A. M. Smith, *Chemical Society Reviews*, 2008, **37**, 664-675.
4. I. Choi, I.-S. Park, J.-H. Ryu and M. Lee, *Chemical Communications*, 2012, **48**, 8481-8483.
5. M. Fandrich, *Cell Mol Life Sci*, 2007, **64**, 2066-2078.
6. J. D. Sipe and A. S. Cohen, *J Struct Biol*, 2000, **130**, 88-98.
7. D. L. Brody, S. Magnoni, K. E. Schweteye, M. L. Spinner, T. J. Esparza, N. Stocchetti, G. J. Zipfel and D. M. Holtzman, *Science*, 2008, **321**, 1221-1224.
8. M. D. Dong, M. B. Hovgaard, W. Mamdouh, S. L. Xu, D. E. Otzen and F. Besenbacher, *Nanotechnology*, 2008, **19**.
9. M. Andreasen, S. B. Nielsen, T. Mittag, M. Bjerring, J. T. Nielsen, S. Zhang, E. H. Nielsen, M. Jeppesen, G. Christiansen, F. Besenbacher, M. Dong, N. C. Nielsen, T. Skrydstrup and D. E. Otzen, *Bba-Proteins Proteom*, 2012, **1824**, 274-285.
10. D. E. Otzen, C. B. Andersen, C. Rischel, M. B. Hovgaard, M. Dong, F. Besenbacher and J. S. Pedersen, *Biophys J*, 2007, 220a-221a.
11. T. Nakagawa, H. Zhu, N. Morishima, E. Li, J. Xu, B. A. Yankner and J. Y. Yuan, *Nature*, 2000, **403**, 98-103.
12. D. Fischer, Y. X. Li, B. Ahlemeyer, J. Krieglstein and T. Kissel, *Biomaterials*, 2003, **24**, 1121-1131.
13. K. Numata and D. L. Kaplan, *Macromol Biosci*, 2011, **11**, 60-64.
14. W. G. Lesniak, M. S. T. Kariapper, B. M. Nair, W. Tan, A. Hutson, L. P. Balogh and M. K. Khan, *Bioconjugate Chem*, 2007, **18**, 1148-1154.
15. S. E. Paramonov, H.-W. Jun and J. D. Hartgerink, *Journal of the American Chemical Society*, 2006, **128**, 7291-7298.
16. C. A. E. Hauser and S. Zhang, *Chemical Society Reviews*, 2010, **39**, 2780-2790.
17. Y. Arii and K. Hatori, *Biochem Bioph Res Co*, 2008, **371**, 772-776.

-
18. W. Qiang, K. Kelley and R. Tycko, *J Am Chem Soc*, 2013, **135**, 6860-6871.
19. L. C. Serpell, *Bba-Mol Basis Dis*, 2000, **1502**, 16-30.
20. S. G. Zhang, *Nat Biotechnol*, 2003, **21**, 1171-1178.
- 5 21. R. Srinivasan, E. M. Jones, K. Liu, J. Ghiso, R. E. Marchant and M. G. Zagorski, *J Mol Biol*, 2003, **333**, 1003-1023.
22. W. G. Hoyer, D. Cherny, V. Subramaniam and T. M. Jovin, *J Mol Biol*, 2004, **340**, 127-139.
- 10 23. W. W. Leow and W. Hwang, *Langmuir*, 2011, **27**, 10907-10913.
24. C. R. So, Y. Hayamizu, H. Yazici, C. Gresswell, D. Khatayevich, C. Tamerler and M. Sarikaya, *Acs Nano*, 2012, **6**, 1648-1656.
- 15 25. W. S. Gosal, I. J. Morten, E. W. Hewitt, D. A. Smith, N. H. Thomson and S. E. Radford, *J Mol Biol*, 2005, **351**, 850-864.
26. A. K. Paravastu, R. D. Leapman, W. M. Yau and R. Tycko, *P Natl Acad Sci USA*, 2008, **105**, 18349-18354.
- 20 27. J. Meinhardt, C. Sachse, P. Hortschansky, N. Grigorieff and M. Fandrich, *J Mol Biol*, 2009, **386**, 869-877.
28. R. Zhang, X. Y. Hu, H. Khant, S. J. Ludtke, W. Chiu, M. F. Schmid, C. Frieden and J. M. Lee, *P Natl Acad Sci USA*, 2009, **106**, 4653-4658.
- 25 29. A. T. Petkova, R. D. Leapman, Z. H. Guo, W. M. Yau, M. P. Mattson and R. Tycko, *Science*, 2005, **307**, 262-265.
30. W. Kim and M. H. Hecht, *P Natl Acad Sci USA*, 2006, **103**, 15824-15829.
- 30 31. C. J. Barrow and M. G. Zagorski, *Science*, 1991, **253**, 179-182.
32. P. Liu, S. Zhang, M. S. Chen, Q. Liu, C. X. Wang, C. Wang, Y. M. Li, F. Besenbacher and M. D. Dong, *Chem Commun*, 2012, **48**, 191-193.
- 35 33. M. B. Hovgaard, M. D. Dong, D. E. Otzen and F. Besenbacher, *Biophys J*, 2007, **93**, 2162-2169.
34. C. M. Dobson, *Nature*, 2003, **426**, 884-890.



The variation in the positions of hydrophobic residues within a peptide sequence can tune the self-assembly
80x40mm (300 x 300 DPI)